

Optimizing 2D-to-3D image conversion for precise flat surface detection using laser triangulation and HSV masking

Bernadeta Siti Rahayu Purwanti¹, Ihsan Auditia Akhinov², Raden Sugeng Mulyono²,
Muhammad Nurtanto², Mustofa Abi Hamid³

¹Department of Electronics Engineering, Politeknik Negeri Jakarta, Depok, Indonesia

²Department of Mechanical Engineering, Politeknik Negeri Jakarta, Depok, Indonesia

³Department of Electrical Engineering Vocational Education, Universitas Sultan Ageng Tirtayasa, Serang, Indonesia

Article Info

Article history:

Received Jul 9, 2024

Revised Sep 10, 2024

Accepted Sep 29, 2024

Keywords:

3D imaging

Digital feature extraction

HSV color

Laser and camera systems

Surface defect detection

Triangulation method

ABSTRACT

This study tackles a critical challenge in converting two-dimensional (2D) images into three-dimensional (3D) representations, focusing on the precise detection of flat surfaces. The research utilizes a triangulation method involving laser and camera systems, emphasizing the optimization of laser shooting angles and camera positioning to accurately determine z-coordinates. The methodology employs hue, saturation, and value (HSV) color masking, which has proven superior to traditional red, green, blue (RGB) methods for isolating red line objects. Key findings indicate that the optimal laser angle, $\beta_1=70.65^\circ$, significantly minimizes root mean square (RMS) error, thereby enhancing the accuracy of 3D imaging. Additionally, the use of three laser lines at different angles enables a more comprehensive detection of z-coordinates by creating multiple reference points across the surface. This arrangement improves the robustness and precision of the 3D reconstruction process, as the intersecting laser lines generate detailed coordinate data that is critical for accurately mapping surface irregularities. These results not only support existing theories in digital feature extraction but also offer a robust framework for practical applications in manufacturing and quality control, particularly in surface defect detection. The study's innovative approach advances the field of computer vision, providing new insights and methodologies for optimizing image conversion techniques.

This is an open access article under the [CC BY-SA](https://creativecommons.org/licenses/by-sa/4.0/) license.



Corresponding Author:

Bernadeta Siti Rahayu Purwanti

Department of Electronics Engineering, Politeknik Negeri Jakarta

Jl. Prof. Dr. G.A. Siwabessy, Kukuasan, Beji, 16425 Depok City, West Java, Indonesia

Email: rahayu.purwanti@elektro.pnj.ac.id

1. INTRODUCTION

In the domain of digital feature extraction [1]–[5], clustering methods based on content similarity [6]–[10] constitute a foundational approach for identifying features within image databases [11]–[15]. Each feature extraction process mathematically translates into a dimensional vector representation, known as a feature vector [16]–[25]. These vectors, derived from image processing and analysis techniques, enable the comparison of different images by analyzing data such as color composition to identify object markings. Despite the extensive research conducted in this field, significant opportunities remain, particularly in detecting concavities in defect detection systems and extracting color images from distance measurement conversions [26].

Continuous improvement in manufacturing product quality is crucial, especially as manufacturers adapt to the challenges posed by big data management [27]. Rapid decision-making based on quality analysis

results is vital for enhancing productivity and sustaining consistent quality in production systems [28]. Effective and prompt decisions rely heavily on accurate analytical methods [29]. Deep learning techniques leveraging big data [30] are increasingly utilized for defect detection in product manufacturing within Industry 4.0 [31]. However, current big data research primarily focuses on data acquisition, preprocessing, processing, and analysis, leaving other critical aspects underexplored [32]–[36]. For example, surface defects on flat surfaces are identified through data evaluation from sensor scans [37]. Eddy current calibration methods analyze sensor excitation frequency, identifying defects such as gaps 1 mm wide and 3 mm deep perpendicular to flat surfaces [38]–[40]. Nevertheless, none of the referenced studies address algorithms for extracting sensor detection results that specifically highlight flat surface defects.

Despite advancements in digital color image extraction, particularly in capturing cross-sectional research objects such as thread diameters [41], a significant gap persists in the literature regarding the detection of defects in adjacent image capture points. Effective interpretation of image data requires extraction processes based on color composition. One color image extraction method [42] employs data clustering by leveraging visual gaps through agglomerative hierarchical clustering (AHC). This approach distinguishes between bottom-up agglomerative methods and top-down divisive methods [43]. Although these hierarchical clustering structures group data based on object color composition, they do not address the detection of adjacent image points as indicators of defects.

Image quality in color object measurements is commonly evaluated using the structural similarity index metric (SSIM), which assesses the similarity between two images on a quantitative scale [44]. Additional quality metrics [45] include mean square error (MSE) and peak signal-to-noise ratio (PSNR). In computer vision, images are partitioned into distinct segments [46], with color pixels analyzed based on nearest-neighbor distances [47] through hierarchical agglomerative methods. Initially, each pixel is treated as an independent cluster, which are then progressively merged with neighboring clusters until a specified cluster count is reached. Although this research covers image quality assessment, evaluation methodologies, algorithms, and clustering techniques for nearest-neighbor groups in images/pixels, it does not address the capture and processing of camera data for defect detection.

This study proposes an innovative approach to defect detection through digital feature extraction using a single camera and three laser lines. Unlike traditional methods that depend on relocating laser points, this method utilizes three laser lines strategically positioned within distinct areas of the camera's capture field. The goal is to improve the efficiency of converting two-dimensional (2D) image masks into three-dimensional (3D) representations without the need to reposition the laser to select data points nearest to the reference point. The reference point is determined by the camera's detection distance to an ideal flat surface, with deviations from this distance indicating defects, such as concave (longer distance) or convex (shorter distance) anomalies. This novel approach addresses existing limitations in defect detection systems, offering a more efficient and accurate method for analyzing surface defects in manufacturing processes. The proposed solution not only enhances the precision of defect detection but also improves the overall efficiency of the quality control process in manufacturing.

2. METHOD

2.1. Experimental setup

The experiments in this study build upon previous research findings, incorporating variations in laser types and camera resolutions [48]. The method for 2D image conversion employed here, utilizing a single laser point and a camera, serves as the foundation of our approach. This method offers several advantages, including simplification of the process through a single laser point and camera setup, which results in cost savings and ease of implementation. Additionally, this method has proven successful in converting electroencephalogram (EEG) signals into image representations for mild depression recognition, demonstrating its effectiveness in signal classification tasks [48]. This underscores the value of innovative approaches when traditional methods face limitations, suggesting that this method, underpinned by deep learning techniques, can enhance performance in complex scenarios. The arrangement of the camera and laser, as depicted in Figure 1, generates a model described by the mathematical (1).

$$Z = \frac{a \cdot z' \cdot \sin(\eta)}{b \cdot \sin(\beta) - z' \cdot \sin(\beta + \eta)} \quad (1)$$

Notes:

z is the object point displacement on the measurand surface

z' is the image point displacement on the charge-coupled device (CCD) sensor

β is the angle between the laser beam and axis of the receiving lens

η is the angle between the CCD sensor and optical axis of the receiving lens
 a is the distance between the camera lens and the laser shot
 b is the distance between the camera lens and CCD array (camera)

2.1.1. Triangulation model diagram

The placement of the camera and CCD sensor, as illustrated in Figure 1, is crucial for achieving accurate focus and effectively capturing the results of laser triangulation [49], [50]. This study modifies the concept depicted in Figure 1(a), which utilizes a single laser point and camera setup, to the arrangement shown in Figure 1(b), where K represents the camera, L1: Laser-1, L2: Laser-2, and L3: Laser-3. Li: 1,2,3 denotes the distances of the camera position relative to the laser's shooting line. The objective is to optimize the dimensional aspects of the images captured by the camera. Similar research has involved projecting laser light onto the object's surface according to the camera lens focus [51], where the height measurement of the object, as captured by the camera, is influenced by the displacement of the laser beam, resulting in a series of points.

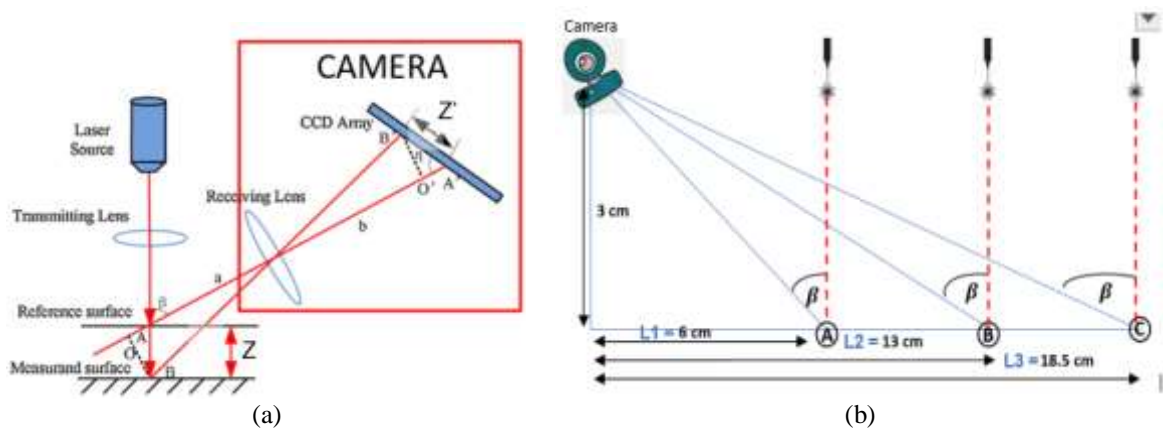


Figure 1. Triangulation model to (a) modification of schematic diagram of the laser triangulation and (b) the setting of camera capture area and laser spotlight

Table 1 presents the experimental configurations used for positioning the camera and laser at various shooting angles. The table includes the height and distance coordinates between the camera and the laser in centimeters, as well as the laser shooting angle (β) in degrees. In the first configuration, the camera is positioned at a height of 3 cm and a distance of 6 cm from the laser, resulting in a shooting angle of $\beta_1=70.65^\circ$. This angle is achieved by maintaining a constant camera height while varying the distance, allowing the laser beams intersecting within the camera's field of view to form a series of coordinate points.

In the second configuration, the camera remains at the same height but is positioned 13 cm away from the laser, producing a shooting angle of $\beta_2=77.05^\circ$. The third configuration shows the camera at a height of 3 cm and a distance of 18.5 cm from the laser, resulting in a shooting angle of $\beta_3=80.78^\circ$. The purpose of these configurations is to demonstrate how varying the distance between the camera and the laser affects the laser shooting angle (β). By keeping the camera height constant, the changes in distance lead to different shooting angles, which is critical for collecting accurate coordinate data (x, y, z) during the 2D to 3D transformation process. This table underscores the significant impact of experimental configuration on the accuracy and detail of 3D surface reconstruction.

Table 1. The placement of camera height and laser line shooting distance

No	Coordinates (height, distance) of laser and camera (cm)	Angle ($^\circ$)	Noted
1	(3, 6)	$\beta_1=70.65$	The variation in angles ($\beta_i, i=1, 2, 3$) is derived from a fixed camera height position (3 cm) while altering the distance. This adjustment causes the intersection of the laser beam lines within the camera's capture area to form a series of points corresponding to the laser beam paths.
2	(3, 13)	$\beta_2=77.05$	
3	(3, 18.5)	$\beta_3=80.78$	

2.1.2. Modified triangulation scheme

According to Figure 1 in the study [48], the original CCD array in the camera was designed to capture the points of incoming light from the laser spot. In this research, the function of the CCD array was modified by incorporating a Logitech Brio Camera. This modification aimed to enable the camera to capture incoming light as it intersects with the laser line.

Other related studies involved capturing road markings using a camera and converting the images into a region of interest (RoI), which highlights the observed object based on the markings captured along the road [52]. The optical system in the laser scanning process reveals the use of laser triangulation sensors. Schlarp *et al.* [53] explains that marking is achieved by adjusting the intensity of the laser light. The marking process involves scanning with laser movement, differing from Kong *et al.* [52], which focused on moving objects. In the latter case, the reflection of the laser beam results from moving objects and is associated with an electric motor.

2.2. Research procedure

The research methodology involves setting the camera position and laser angle to acquire coordinate points (pixels) for marking. A series of markings are identified (marked) by selecting only the red pixels. The masking results reveal the coordinates of the examined object, specifically a flat surface. Li *et al.* [48] concept, any unevenness on the flat surface indicates concave or convex point coordinates. These concave or convex coordinates are derived by comparing the pixel coordinates captured by the camera with the laser scan results against reference coordinates. The reference coordinates are based on data captured by the camera and the ideal coordinates (x, y) , which produce new coordinates that form a three-dimensional image (x, y, z) . The data processing of the captured images intersects with the laser scan results, forming a series of points using OpenCV-Python [54], [55]. This data processing involves conversion results and color selection based on pixel coordinate references for comparison. Differences in pixel values compared to reference points indicate anomalies or coordinate mismatches, which suggest the height of the object, whether concave or convex.

2.3. Data acquisition and testing

To ensure scientific rigor and acceptance, the research provides a comprehensive and detailed description of the experimental methods. The camera and lasers are strategically positioned at specific angles to capture the necessary coordinates. Red pixels are tagged, and masking techniques are applied to emphasize the object's coordinates, which are subsequently compared with reference coordinates to identify concave or convex points. Data is meticulously processed using OpenCV-Python to analyze and detect anomalies or mismatches, ensuring the accuracy and reliability of the results. This systematic approach, from precise experimental setup to detailed data analysis, ensures the validity and accuracy of the 3D surface reconstruction, thereby making the findings robust and scientifically credible.

3. RESULTS AND DISCUSSION

3.1. Implementation trial concept

The execution of this research follows the logic depicted in Figure 2. The execution is as follows: from a 2D image with column (x) and row (y) information, it is transformed into a 3D image to form coordinates (x, y, z) , where z is obtained from engineering the coordinates (x, y) [56], [57]. The experimental procedure using the triangulation method with a laser involves several key stages. First, the camera and laser positions are set according to the camera's capture area, with three different position laser heights and distance: (3, 6), (3, 13), and (3, 18.5) in Table 1. Second, data marking and masking are performed by identifying red pixels and applying masking to emphasize the object coordinates. The masking process in OpenCV generates coordinates (x, y) with the origin at $(0, 0)$, allowing the coordinates of the processed 2D image to be identified. Third, coordinate comparison is carried out by comparing the captured coordinates with the reference coordinates to determine concave or convex points. Finally, data processing is conducted using OpenCV-python to analyze the data, identify anomalies, and correct mismatches. This process ensures accurate and reliable results in converting 2D images into comprehensive and detailed 3D models.

3.2. Algorithm programming

The algorithm for processing 2D images into 3D involves using line lasers to detect changes in laser markings when encountering a flat object's surface. The 2D images captured by the camera are converted into hue, saturation, and value (HSV) color space, and the data conversion process is conducted using OpenCV. Transforming 2D images into 3D includes engineering a series of marking points and masking the red color as a reference. Masking results from these marked points, with coordinates (x, y) selected along the red line.

Measurements are categorized into those close to the reference coordinates and those with significant deviations from the reference.

The process, outlined in the flowchart in Figure 3, involves several steps for object extraction and 3D reconstruction. Initially, images of a flat object's surface are captured using a camera, followed by data collection from both camera captures and laser line scanning to obtain point coordinates [18]. The collected data is then sorted or masked based on color using the HSV method to isolate red objects from other colors on the same object [36], [57]–[63]. This color-based sorting helps identify the series of points forming the red line on the flat object's surface, serving as a reference.

Subsequent steps involve identifying reference points that show anomalies from the reference line, distinguishing the coordinates of a flat test object from the reference line to determine concavity or convexity, and calculating the z coordinate using a triangulation algorithm to introduce a third dimension. By comparing the surface coordinates of the test object with the reference line, pixel differences are computed to derive the z coordinate, thereby transforming the object into a 3D representation. Finally, XYZ coordinates are obtained based on the logic in Figure 3, enabling the visualization of 3D images of objects that either match or deviate from the reference.

The utilization of the HSV method in the color-based sorting process is crucial for accurately extracting red objects from the background, enhancing the precision of the subsequent 3D reconstruction process [36], [57], [64]. By leveraging the strengths of color-based methods and integrating them into the object extraction and 3D reconstruction workflow, researchers can achieve more accurate and detailed representations of objects, particularly in scenarios where color plays a significant role in distinguishing features.

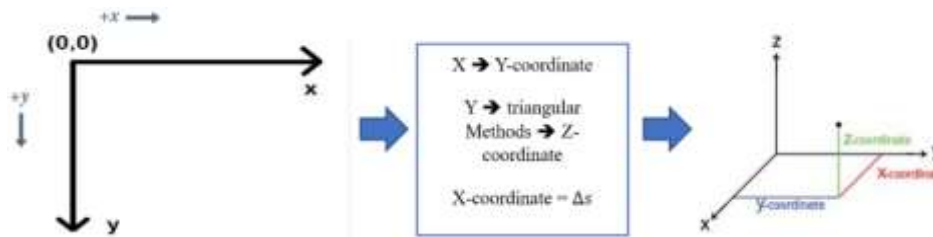


Figure 2. Logic of engineering 2D into 3D

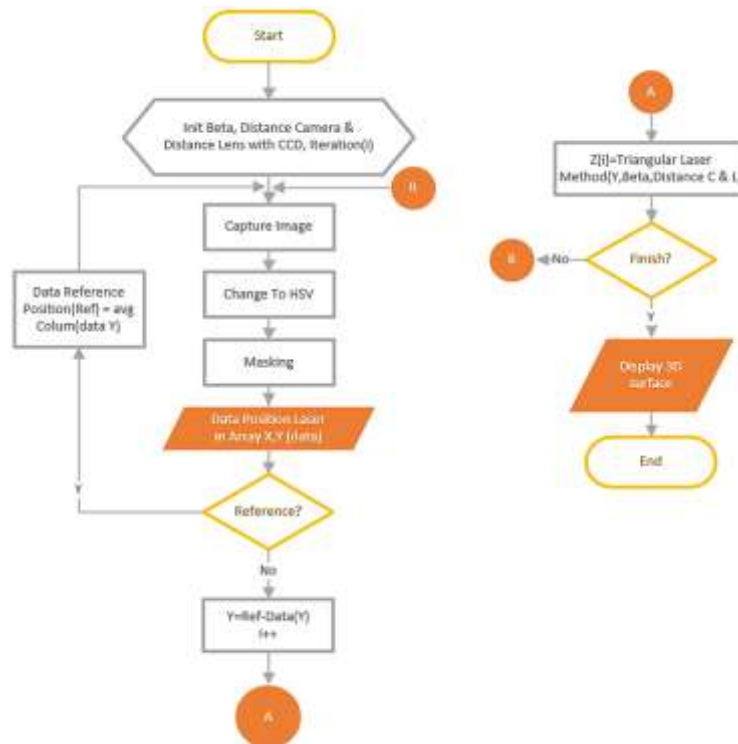


Figure 3. Flowchart of triangular methods

3.3. The flat surface as test object

Flat surface objects with uniform dimensions (width=4 cm, thickness=1 cm, length=2 cm) generate coordinate point markings when images are captured by the camera as shown in Figure 4. To convert these 2D images into 3D representations, the triangulation method is applied to the captured 2D images. A single image capture only provides the two-dimensional surface of the flat object, represented by coordinates (x, y). Therefore, multiple image captures are necessary to establish the three-dimensional coordinates (x, y, z).

The 3D image is obtained by converting the color data from the 2D image captured by the camera into spatial coordinates. This conversion process generates coordinate points, which are refined through distance shifting to achieve accurate pixelation of the image data. The shift distance per segment is set at $n=0.5$ cm, allowing for precise selection of red pixels along the laser line as shown in Figure 5.

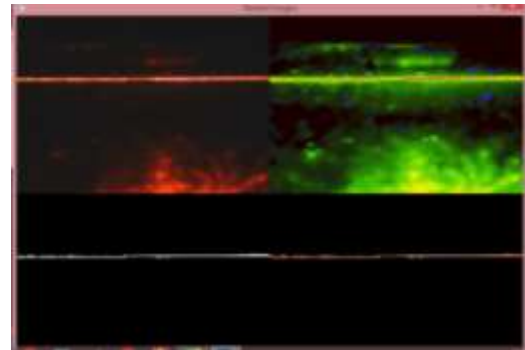
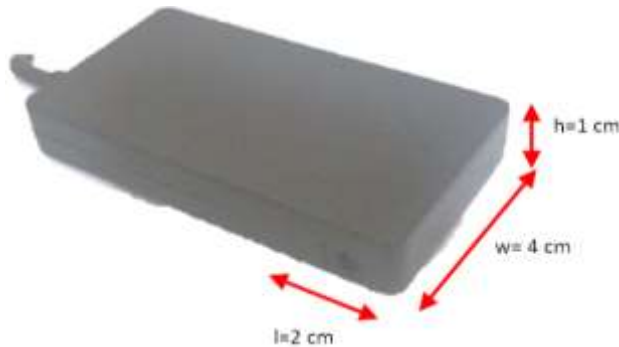


Figure 4. Flat surface as testing object for 3D illustration

Figure 5. The result of red color masking using HSV

Color-based object extraction has been extensively researched in the field of computer vision. Various color spaces, such as HSV and red, green, blue (RGB), have been explored to enhance the accuracy of object extraction. The integration of HSV and RGB methods has demonstrated superior results in object extraction [65]. Notably, the HSV method has been regarded as more effective than RGB in these tasks [66]. This preference for the HSV method stems from its closer alignment with the human visual system, making it more efficient in extracting primary colors from the background [66]. Masking involves sorting images based on color according to specified parameters (HSV) and/or base colors (RGB). To obtain HSV color characteristics, a color conversion process is carried out from RGB to HSV as seen in Figure 6. After normalizing the RGB image, it is then converted into an HSV image.

Research has underscored the critical role of color in various computer vision tasks, including object detection, segmentation, and tracking. When combined with other features, such as texture and depth information, color features have been shown to enhance the performance of object detection and tracking. Furthermore, color histograms have proven to be effective cues for indexing colorful objects in large databases, highlighting the strength of color-based approaches in image retrieval tasks [67]. Consequently, this study concludes that the HSV method outperforms RGB in object extraction. Variations in HSV parameters significantly influence the clarity of the red line object. Figure 6(a) depicts the initial results of red color masking using the HSV method with parameters $H=0-19$, $S=110-240$, $V=153-255$. The red color is detected quite well, but some interference from similar colors persists. Subsequently, Figure 6(b) illustrates the results of modifying the HSV parameters to $H=0-179$, $S=110-240$, $V=153-255$. The detection of the red color becomes more extensive, yet there remains some background interference. Figure 6(c) employs HSV parameters $H=0-179$, $S=54-240$, $V=153-255$, with detection results showing an improvement in the red area, though slight interference is still present. Conversely, Figure 6(d) with parameters $H=0-179$, $S=0-255$, $V=252-255$, exhibits very clear red color detection with significantly reduced background interference. Finally, Figure 6(e) demonstrates the best results using HSV parameters $H=0-179$, $S=0-255$, $V=224-255$, where the red area is detected exceptionally well without background interference. These images conclusively show that variations in HSV parameters critically impact the clarity and accuracy of red object detection. The optimal parameters were identified as $H=0-179$, $S=0-255$, and $V=224-255$, yielding the best detection results with minimal background interference. This range of minimum-maximum HSV values serves as the foundation for selecting color masking values in subsequent experiments.

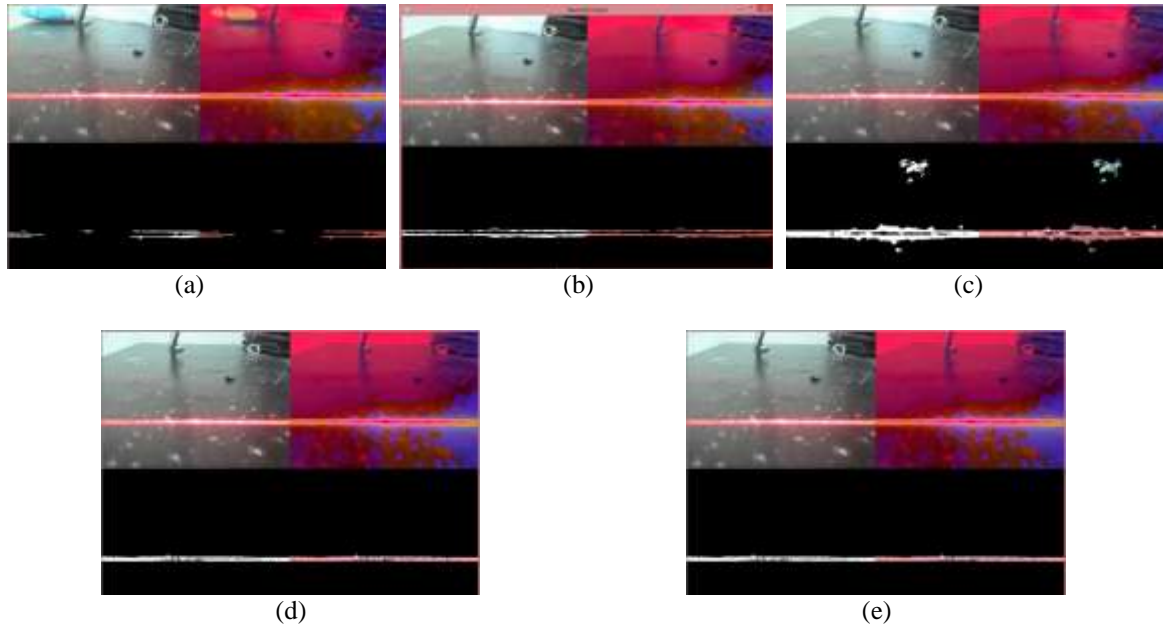


Figure 6. Red color masking results using HSV: (a) red color detection is quite good, (b) red color detection is more extensive, (c) red color detection is more extensive with improvements, (d) red color detection is very clear, and (e) red color detection is excellent without interference

3.4. Test results

The number of marking lines in Figure 7 varies with each shooting angle, within a sample range of 0-100. For the x-coordinate where the pixel value is 0, the corresponding y-coordinate count at that point is 6, with subsequent x-coordinates showing inconsistency in the number of y-coordinates. In the context of object extraction and 3D reconstruction, such data fluctuations can significantly affect the accuracy of reference point determination using the triangle method. To mitigate these fluctuations, it is crucial to implement an averaging system for each pixel coordinate when forming marker points (x, y, z) [68]. This averaging approach stabilizes the data, reduces the impact of variations, and enhances the reliability of reference points in the reconstruction process as shown in Figure 8. Furthermore, the selection of red coordinate conversion results as reference points should be tested under varying ambient light intensities to ensure stability and consistency [69]. The influence of ambient light intensity on the stability of the laser line, as shown in Figure 8, indicates potential instability under different lighting conditions, such as 25 lux, 50 lux, and 64 lux. Ideally, reference coordinates should remain stable, which necessitates either conditioning the test chamber to exclude light or considering the use of a laser type with adjustable intensity to address this issue.

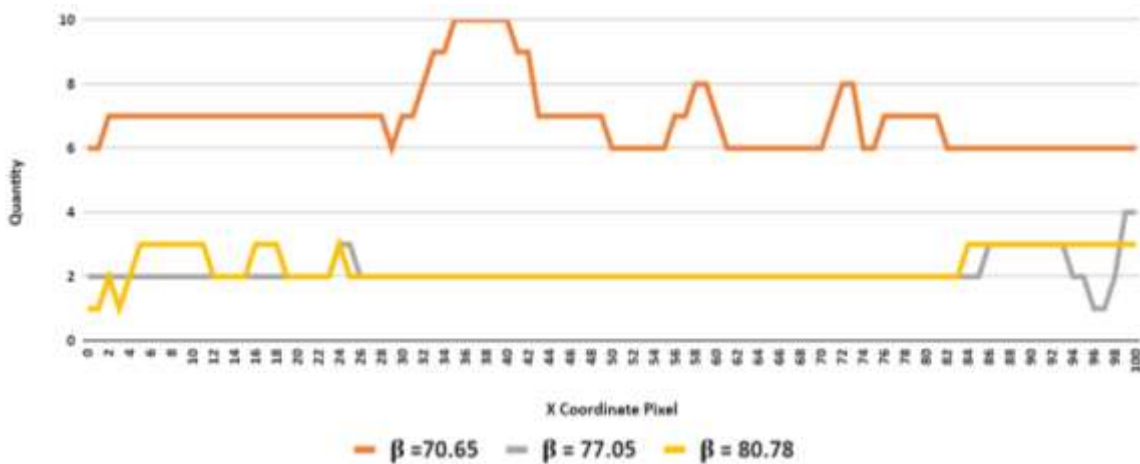


Figure 7. The number of pixels detected based on the camera shooting angle

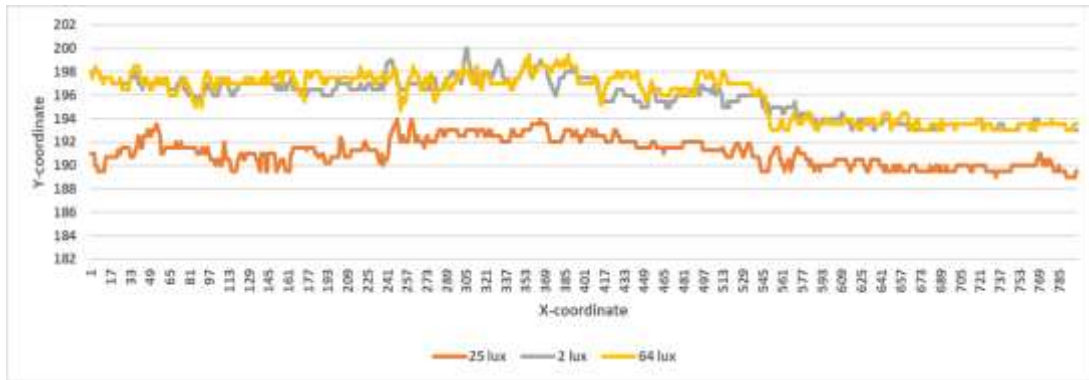


Figure 8. The reference point array as reference coordinates based on changes in light intensity

The 3D surface marking and masking results in Figure 9 illustrate the influence of varying laser shooting angles on the accuracy and detail of 3D reconstructions. At $\beta_1=70.65^\circ$ (Figures 9(a) and 9(b)), the marking lines are distinct, and the 3D surface is well-defined, leading to optimal pixel detection and a highly detailed reconstruction. This narrower shooting angle facilitates a higher number of detected pixels, thereby enhancing the precision of the 3D model [61]-[70]. In contrast, at $\beta_2=77.05^\circ$ (Figures 9(c) and 9(d)), the marking lines are less dense, indicating fewer detected pixels and a slight reduction in surface detail. At $\beta_3=80.78^\circ$ (Figures 9(e) and 9(f)), the marking lines become sparse, resulting in the least detailed 3D surface and the lowest number of detected pixels. As the shooting angle increases, pixel detection decreases, which negatively impacts HSV color classification and z-coordinate determination, leading to less accurate 3D reconstructions. Variations in external light can cause intensity discrepancies between reference and test data, thereby affecting the accuracy of z-axis calculations. To mitigate this, tests are conducted in a controlled lighting environment at 2 lux. The optimal angle, $\beta_1=70.65^\circ$, yields the most accurate results with the smallest average root mean square (RMS) error, offering the best balance between detail and precision [71]. These findings underscore the critical importance of selecting an appropriate laser shooting angle and maintaining consistent external lighting conditions to achieve accurate and detailed 3D reconstructions.

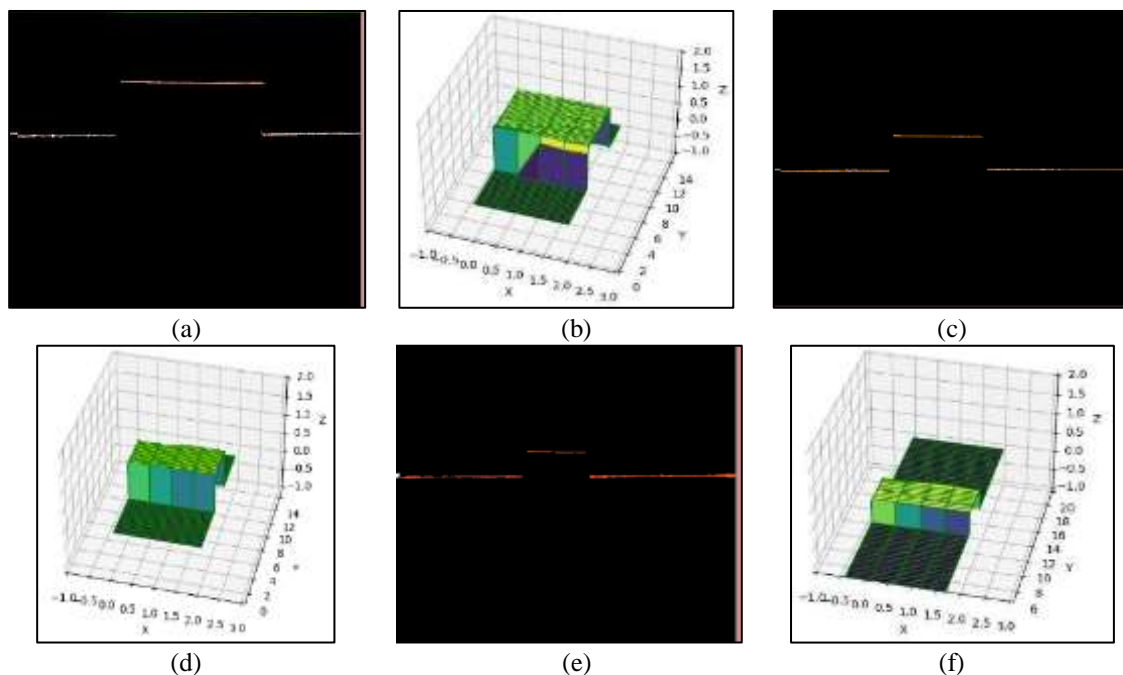


Figure 9. Results of variations on 3D surfaces: (a) marker line at angle $\beta_1=70.65^\circ$, (b) pixel detection at angle $\beta_1=70.65^\circ$, (c) marker line at angle $\beta_2=77.05^\circ$, (d) pixel detection with angle $\beta_2=77.05^\circ$, (e) marker line at angle $\beta_3=80.78^\circ$, and (f) pixel detection with angle $\beta_3=80.78^\circ$

The smallest average RMS error for object height and width was achieved at $\beta_1=70.65^\circ$, ensuring accurate z-coordinate determination. This selection is grounded in test data and simulations conducted using the OpenCV program. While OpenCV offers limited features in responding to instructions, its performance is also impacted by the accuracy of image capture sharpness [54]. This research has successfully met its objectives and can be further advanced by incorporating instruments or software that offer greater compatibility. Future developments should focus on enhancing image capture sharpness (pixels) and expanding the simulator's feature set to provide more comprehensive instructional capabilities.

Based on Table 2, the smallest average RMS error for height and width was achieved at $\beta_1=70.65^\circ$, providing accurate z-coordinate measurements. This selection is supported by test and simulation data within the OpenCV program [54], where image sharpness accuracy and the program's limited response to instructions played significant roles. The research has successfully met its objectives and can be further refined by adopting more compatible instruments or software. Future enhancements should focus on achieving sharper image capture (pixels) and expanding the simulator's feature set to offer more comprehensive instructional capabilities.

Table 2. The calculation results of coordinate points for the z and y axes with variations in the laser shooting angle (β°)

Segment	The reference average height -z (cm)	Z-coordinate (cm)					
		$\beta_1=70.65$	$\beta_2=77.05$	$\beta_3=80.78$	$\beta_1=70.65$	$\beta_2=80.78$	$\beta_3=80.78$
0	1	1.17	0.78	0.50	0.17	0.22	0.52
1		1.17	0.78	0.49	0.17	0.22	0.53
2		1.18	0.81	0.49	0.18	0.19	0.53
3		1.17	0.81	0.49	0.17	0.19	0.53
4		1.18	0.81	0.49	0.18	0.19	0.53
5		1.17	0.78	0.50	0.17	0.22	0.52
	Average	1.17	0.80	0.49	0.17	0.21	0.53
0	4	3.90	3.79	3.79	0.10	0.21	0.21
1		3.90	3.79	3.79	0.10	0.21	0.21
2		3.90	3.79	3.79	0.10	0.21	0.21
3		3.90	3.79	3.79	0.10	0.21	0.21
4		3.90	3.79	3.79	0.10	0.21	0.21
5		3.90	3.79	3.79	0.10	0.21	0.21
	Average	3.90	3.79	3.79	0.10	0.21	0.21

4. CONCLUSION

This study successfully implemented a triangulation method utilizing laser and camera systems to convert 2D images into 3D representations. The findings demonstrate that adjusting laser shooting angles and camera positions is crucial for accurately determining z-coordinates, thereby enabling precise 3D imaging of flat surfaces. The optimal laser angle, yielding the smallest RMS error, was identified as $\beta_1=70.65^\circ$, corroborating the method's accuracy and consistency with previous research. Additionally, the study confirms that the HSV color masking method outperforms the RGB method in object extraction, particularly in effectively isolating red line objects. These results align with existing literature, deepening the understanding of digital feature extraction and providing a robust framework for future research in this domain. This research advances the scientific knowledge of 3D imaging techniques, offering practical applications for manufacturing and quality control processes that demand precise surface defect detection. The study supports existing theories while introducing new insights into optimizing image conversion methods, thereby making a significant contribution to the fields of computer vision and digital feature extraction.

REFERENCES

- [1] D. N. Hire, A. V. Patil, and P. Charles, "Efficient rotated and scaled digital image retrieval model using deep learning-based hybrid features extraction," *Multimedia Tools and Applications*, vol. 83, no. 12, pp. 34733–34758, Sep. 2023, doi: 10.1007/s11042-023-17016-y.
- [2] T. Li, "A digital cultural heritage tourism information statistics system based on image feature extraction technology," *Computer-Aided Design and Applications*, vol. 21, no. S16, pp. 1–18, Jan. 2024, doi: 10.14733/cadaps.2024.S16.1-18.
- [3] Y. Liang, M. C. Fairhurst, R. M. Guest, and M. Erbilek, "Automatic handwriting feature extraction, analysis and visualization in the context of digital palaeography," *International Journal of Pattern Recognition and Artificial Intelligence*, vol. 30, no. 04, p. 1653001, May 2016, doi: 10.1142/S0218001416530013.
- [4] C. Shan, S. Zhou, Z. Zhang, and M. Li, "Digital watermarking method for image feature point extraction and analysis," *International Journal of Intelligent Systems*, vol. 37, no. 10, pp. 7281–7299, Oct. 2022, doi: 10.1002/int.22881.





- [5] J. Li, "Research on image texture feature extraction based on digital twin," *Mathematical Problems in Engineering*, vol. 2022, no. 1, p. 6788719, Jun. 2022, doi: 10.1155/2022/6788719.
- [6] S. Mahajan and D. Patil, "Image retrieval using contribution-based clustering algorithm with different feature extraction techniques," in *2014 Conference on IT in Business, Industry and Government (CSIBIG)*, 2014, pp. 1–7. doi: 10.1109/CSIBIG.2014.7057001.
- [7] A. Meenakshi, A. P. Janani, S. D. Mahalakshmi, and S. V. Sivagami, "A novel image recognition using Fuzzy C-Means and content-based fabric image retrieval," *The Imaging Science Journal*, vol. 71, no. 5, pp. 395–407, Jul. 2023, doi: 10.1080/13682199.2023.2183316.
- [8] G. Wei, H. Ma, W. Qian, and M. Qiu, "Similarity measurement of lung masses for medical image retrieval using kernel based semisupervised distance metric," *Medical Physics*, vol. 43, no. 12, pp. 6259–6269, Dec. 2016, doi: 10.1118/1.4966030.
- [9] H. Bi, Y. Jiang, H. Tang, G. Yang, H. Shu, and J.-L. Dillenseger, "Fast and accurate segmentation method of active shape model with Rayleigh mixture model clustering for prostate ultrasound images," *Computer Methods and Programs in Biomedicine*, vol. 184, p. 105097, Feb. 2020, doi: 10.1016/j.cmpb.2019.105097.
- [10] Z. S. Younus *et al.*, "Content-based image retrieval using PSO and k-means clustering algorithm," *Arabian Journal of Geosciences*, vol. 8, no. 8, pp. 6211–6224, 2015, doi: 10.1007/s12517-014-1584-7.
- [11] Z. Qi, "English sentence semantic feature extraction method based on fuzzy logic algorithm," *Journal of Electrical Systems*, vol. 20, no. 1, pp. 262–275, 2024, doi: 10.52783/jes.681.
- [12] G. Sucharitha, N. Arora, and S. C. Sharma, "Medical image retrieval using a novel local relative directional edge pattern and Zernike moments," *Multimedia Tools and Applications*, vol. 82, no. 20, pp. 31737–31757, Aug. 2023, doi: 10.1007/s11042-023-14720-7.
- [13] S. M. Islam, M. Banerjee, S. Bhattacharyya, and S. Chakraborty, "Content-based image retrieval based on multiple extended fuzzy-rough framework," *Applied Soft Computing*, vol. 57, pp. 102–117, Aug. 2017, doi: 10.1016/j.asoc.2017.03.036.
- [14] N. Vretos, V. Solachidis, and I. Pitas, "A mutual information based face clustering algorithm for movie content analysis," *Image and Vision Computing*, vol. 29, no. 10, pp. 693–705, Sep. 2011, doi: 10.1016/j.imavis.2011.07.006.
- [15] K. Juneja, "Multi-featured and fuzzy based dual analysis approach to optimize the subspace clustering for images," *Wireless Personal Communications*, vol. 114, no. 3, pp. 2417–2447, Oct. 2020, doi: 10.1007/s11277-020-07482-0.
- [16] G. Kataoka, M. Yamamoto, M. Inagi, S. Nagayama, and S. Wakabayashi, "Feature vectors based on wire width and distance for lithography hotspot detection," *IPSI Transactions on System and LSI Design Methodology*, vol. 16, pp. 2–11, 2023, doi: 10.2197/ipsjtsldm.16.2.
- [17] Bobbinpreet *et al.*, "MRMR based feature vector design for efficient citrus disease detection," *Computers, Materials & Continua*, vol. 72, no. 3, pp. 4771–4787, 2022, doi: 10.32604/cmc.2022.023150.
- [18] L. Zhang, S. Wang, C. Liu, and Y. Wang, "Saliency-driven oil tank detection based on multidimensional feature vector clustering for SAR images," *IEEE Geoscience and Remote Sensing Letters*, vol. 16, no. 4, pp. 653–657, Apr. 2019, doi: 10.1109/LGRS.2018.2878106.
- [19] D.-H. Yang, H.-L. Gu, T.-H. Yi, and H.-N. Li, "Bridge cable anomaly detection based on local variability in feature vector of monitoring group cable forces," *Journal of Bridge Engineering*, vol. 28, no. 6, p. 04023030, Jun. 2023, doi: 10.1061/JBENF2.BEENG-6084.
- [20] D. Desmira, N. Abu Bakar, R. Wiryadinata, M. Abi Hamid, N. Kholifah, and M. Nurtanto, "Comparison of principal component analysis and ANFIS to improve EEEV Laboratory energy use prediction performance," *Indonesian Journal of Electrical Engineering and Computer Science (IJECS)*, vol. 27, no. 2, pp. 970–979, Aug. 2022, doi: 10.11591/ijeecs.v27.i2.pp970-979.
- [21] J. Liu and E. Zio, "Feature vector regression with efficient hyperparameters tuning and geometric interpretation," *Neurocomputing*, vol. 218, pp. 411–422, Dec. 2016, doi: 10.1016/j.neucom.2016.08.093.
- [22] J. Park and J. Kim, "Emotional information processing based on feature vector enhancement and selection for human-computer interaction via speech," *Telecommunication Systems*, vol. 60, no. 2, pp. 201–213, Oct. 2015, doi: 10.1007/s11235-015-0023-8.
- [23] Q. Ni *et al.*, "A Feature vector learning-based method for diagnosing main circuit ground faults in electrical traction drive systems," *IEEE Transactions on Power Electronics*, vol. 39, no. 2, pp. 2537–2545, Feb. 2024, doi: 10.1109/TPEL.2023.3326712.
- [24] M. P. Kumar and M. K. Rajagopal, "Detecting facial emotions using normalized minimal feature vectors and semi-supervised twin support vector machines classifier," *Applied Intelligence*, vol. 49, no. 12, pp. 4150–4174, Dec. 2019, doi: 10.1007/s10489-019-01500-w.
- [25] C. He, X. Huo, and H. Gao, "FT-FVC: fast transformation-based feature vector concatenation for time series classification," *Applied Intelligence*, vol. 53, no. 14, pp. 17778–17795, Jul. 2023, doi: 10.1007/s10489-022-04386-3.
- [26] J. Li, Q. Sun, K. Chen, H. Cui, K. Huangfu, and X. Chen, "3D large-scale point cloud semantic segmentation using optimal feature description vector network: OFDV-Net," *IEEE Access*, vol. 8, pp. 226285–226296, 2020, doi: 10.1109/ACCESS.2020.3044166.
- [27] J. Wang and B. Liu, "Analyzing the feature extraction of football player's offense action using machine vision, big data, and internet of things," *Soft Computing*, vol. 27, no. 15, pp. 10905–10920, Aug. 2023, doi: 10.1007/s00500-023-08735-3.
- [28] L. Da Xu, E. L. Xu, and L. Li, "Industry 4.0: state of the art and future trends," *International Journal of Production Research*, vol. 56, no. 8, pp. 2941–2962, Apr. 2018, doi: 10.1080/00207543.2018.1444806.
- [29] R. S. Peres, X. Jia, J. Lee, K. Sun, A. W. Colombo, and J. Barata, "Industrial Artificial Intelligence in Industry 4.0 - Systematic Review, Challenges and Outlook," *IEEE Access*, vol. 8, pp. 220121–220139, 2020, doi: 10.1109/ACCESS.2020.3042874.
- [30] A. Abou Tabl, A. Alkhateeb, and W. ElMaraghy, "Deep learning method based on big data for defects detection in manufacturing systems industry 4.0," *International Journal of Industry and Sustainable Development*, vol. 2, no. 1, pp. 1–14, Jan. 2021, doi: 10.21608/ijisd.2021.145552.
- [31] R. Muniappan *et al.*, "Optimizing feature extraction for tampering image detection using deep learning approaches," *Indonesian Journal of Electrical Engineering and Computer Science*, vol. 35, no. 3, pp. 1853–1864, 2024, doi: 10.11591/ijeecs.v35.i3.pp1853-1864.
- [32] X. Xu and Q. Hua, "Industrial big data analysis in smart factory: current status and research strategies," *IEEE Access*, vol. 5, pp. 17543–17551, 2017, doi: 10.1109/ACCESS.2017.2741105.
- [33] R. F. Babiceanu and R. Seker, "Big Data and virtualization for manufacturing cyber-physical systems: A survey of the current status and future outlook," *Computers in Industry*, vol. 81, pp. 128–137, Sep. 2016, doi: 10.1016/j.compind.2016.02.004.
- [34] D. Desmira, N. A. Bakar, M. R. Hashim, R. Wiryadinata, and M. A. Hamid, "Laboratory prediction energy control system based on artificial intelligence network," *Bulletin of Electrical Engineering and Informatics (BEEI)*, vol. 11, no. 3, pp. 1280–1288, Jun. 2022, doi: 10.11591/eei.v11i3.1821.
- [35] D. Desmira, M. A. Hamid, N. A. Bakar, M. Nurtanto, and S. Sunardi, "A smart traffic light using a microcontroller based on the fuzzy logic," *IAES International Journal of Artificial Intelligence (IJ-AI)*, vol. 11, no. 3, pp. 809–818, Sep. 2022, doi: 10.11591/ijai.v11.i3.pp809-818.

- [36] Y. Huang, Y. Xu, X. Fang, and B. Wei, "Current status, future developments and recent patents on big data technique in process control systems," *Recent Patents on Mechanical Engineering*, vol. 9, no. 2, pp. 112–124, May 2016, doi: 10.2174/2212797609666160413161049.
- [37] J. W. Park *et al.*, "Rail surface defect detection and analysis using multi-channel eddy current method based algorithm for defect evaluation," *Journal of Nondestructive Evaluation*, vol. 40, no. 3, p. 83, Sep. 2021, doi: 10.1007/s10921-021-00810-9.
- [38] M. Schwerter, M. Zimmermann, J. Felder, and N. J. Shah, "Efficient eddy current characterization using a 2D image-based sampling scheme and a model-based fitting approach," *Magnetic Resonance in Medicine*, vol. 85, no. 5, pp. 2892–2903, 2021, doi: 10.1002/mrm.28597.
- [39] J. Forbriger and F. Stefani, "Transient eddy current flow metering," *Measurement Science and Technology*, vol. 26, no. 10, p. 105303, Oct. 2015, doi: 10.1088/0957-0233/26/10/105303.
- [40] D. Desmira, M. A. Hamid, Irwanto, S. D. Ramdani, and T. Y. Pratama, "An ultrasonic and temperature sensor prototype using fuzzy method for guiding blind people," *Journal of Physics: Conference Series*, vol. 1446, no. 1, p. 012045, Jan. 2020, doi: 10.1088/1742-6596/1446/1/012045.
- [41] F. Firdaus, E. Rachmawati, and F. Sthevanie, "Hybrid approach for fruit recognition in high data variance," in *AIP Conference Proceedings*, 2020, vol. 2233, p. 030003, doi: 10.1063/5.0001362.
- [42] T. A. Munandar and D. Handayani, "Extracting patterns of proximity in regional development inequality using hierarchical agglomerative clustering," *TEM Journal*, vol. 12, no. 2, pp. 680–690, May 2023, doi: 10.18421/TEM122-11.
- [43] M. Kashyap, S. Gogoi, R. Kumar Prasad, and A. Professor, "A comparative study on partition-based clustering methods," *International Journal of Creative Research Thoughts*, vol. 6, no. 2, pp. 2320–2882, 2018, [Online]. Available: www.ijcrt.org.
- [44] M. M. Petrou and S. Kamata, *Image processing: dealing with texture*. United Kingdom: John Wiley & Sons, 2021.
- [45] A. Munshi *et al.*, "Image compression using K-mean clustering algorithm," *International Journal of Computer Science & Network Security*, vol. 21, no. 9, pp. 275–280, 2021.
- [46] R. Parihar, S. Sawhney, A. Vaish, and S. Verma, "Image processing using K means clustering and euclidean distance method," *International Journal of Technical Research & Science*, vol. VII, no. III, pp. 1–15, Mar. 2022, doi: 10.30780/ijtrs.v07.i03.001.
- [47] P. M. Prihatini, I. K. G. D. Putra, I. A. D. Giriantari, and M. Sudarma, "Complete agglomerative hierarchy document's clustering based on fuzzy luhn's gibbs latent dirichlet allocation," *International Journal of Electrical and Computer Engineering (IJECE)*, vol. 9, no. 3, pp. 2103–2111, Jun. 2019, doi: 10.11591/ijece.v9i3.pp2103-2111.
- [48] S. Li, X. Jia, M. Chen, and Y. Yang, "Error analysis and correction for color in laser triangulation measurement," *Optik*, vol. 168, pp. 165–173, Sep. 2018, doi: 10.1016/j.ijleo.2018.04.057.
- [49] V. Meana, P. Zapico, E. Cuesta, S. Giganto, and S. Martinez-Pellitero, "Laser triangulation sensors performance in scanning different materials and finishes," *Sensors*, vol. 24, no. 8, p. 2410, Apr. 2024, doi: 10.3390/s24082410.
- [50] L. Hua, Y. Lu, J. Deng, Z. Shi, and D. Shen, "3D reconstruction of concrete defects using optical laser triangulation and modified spacetime analysis," *Automation in Construction*, vol. 142, p. 104469, Oct. 2022, doi: 10.1016/j.autcon.2022.104469.
- [51] G. Ye *et al.*, "Improving measurement accuracy of laser triangulation sensor via integrating a diffraction grating," *Optics and Lasers in Engineering*, vol. 143, p. 106631, Aug. 2021, doi: 10.1016/j.optlaseng.2021.106631.
- [52] W. Kong, T. Zhong, X. Mai, S. Zhang, M. Chen, and G. Lv, "Automatic detection and assessment of pavement marking defects with street view imagery at the city scale," *Remote Sensing*, vol. 14, no. 16, p. 4037, Aug. 2022, doi: 10.3390/rs14164037.
- [53] J. Schlarp, E. Csencsics, and G. Schitter, "Design and evaluation of an integrated scanning laser triangulation sensor," *Mechatronics*, vol. 72, p. 102453, Dec. 2020, doi: 10.1016/j.mechatronics.2020.102453.
- [54] H. Varçin, F. Üneş, E. Gemici, and M. Zelenakova, "Development of a three-dimensional CFD model and OpenCV code by comparing with experimental data for spillway model studies," *Water*, vol. 15, no. 4, p. 756, Feb. 2023, doi: 10.3390/w15040756.
- [55] M. A. Hamid, D. Aditama, E. Permata, N. Kholifah, M. Nurtanto, and N. W. Abdul Majid, "Simulating the Covid-19 epidemic event and its prevention measures using python programming," *Indonesian Journal of Electrical Engineering and Computer Science (IJECS)*, vol. 26, no. 1, pp. 278–288, Apr. 2022, doi: 10.11591/ijeecs.v26.i1.pp278-288.
- [56] G. Fu, A. Menciasci, and P. Dario, "Development of a low-cost active 3D triangulation laser scanner for indoor navigation of miniature mobile robots," *Robotics and Autonomous Systems*, vol. 60, no. 10, pp. 1317–1326, Oct. 2012, doi: 10.1016/j.robot.2012.06.002.
- [57] J. Chen, D. Wu, P. Song, F. Deng, Y. He, and S. Pang, "Multi-View triangulation: systematic comparison and an improved method," *IEEE Access*, vol. 8, pp. 21017–21027, 2020, doi: 10.1109/ACCESS.2020.2969082.
- [58] P. Flores-Vidal, D. Gómez, J. Castro, and J. Montero, "New aggregation approaches with HSV to color edge detection," *International Journal of Computational Intelligence Systems*, vol. 15, no. 1, pp. 1–15, 2022, doi: 10.1007/s44196-022-00137-x.
- [59] B. Hdouid, M. E. H. Tirari, R. O. H. Thami, and R. Faizi, "Detecting and shadows in the HSV color space using dynamic thresholds," *International Journal of Electrical and Computer Engineering (IJECE)*, vol. 8, no. 3, pp. 1513–1521, 2018, doi: 10.11591/ijece.v8i3.pp1513-1521.
- [60] Y. Ito, C. Premachandra, S. Sumathipala, H. W. H. Premachandra, and B. S. Sudantha, "Tactile Paving detection by dynamic thresholding based on HSV space analysis for developing a walking support system," in *IEEE Access*, 2021, pp. 20358–20367, doi: 10.1109/ACCESS.2021.3055342.
- [61] V. Chernov, J. Alander, and V. Bochko, "Integer-based accurate conversion between RGB and HSV color spaces," *Computers and Electrical Engineering*, vol. 46, pp. 328–337, 2015, doi: 10.1016/j.compeleceng.2015.08.005.
- [62] S. Kim and J. You, "Efficient LUT design methodologies of transformation between RGB and HSV for HSV based image enhancements," *Journal of Electrical Engineering and Technology*, vol. 19, no. 7, pp. 4551–4563, 2024, doi: 10.1007/s42835-024-01859-y.
- [63] P. Flores-Vidal, D. Gómez, J. Castro, and J. Montero, "New aggregation approaches with HSV to color edge detection," *International Journal of Computational Intelligence Systems*, vol. 15, no. 1, p. 78, Sep. 2022, doi: 10.1007/s44196-022-00137-x.
- [64] C. Li *et al.*, "An underwater image enhancement benchmark dataset and beyond," *IEEE Transactions on Image Processing*, vol. 29, pp. 4376–4389, 2020, doi: 10.1109/TIP.2019.2955241.
- [65] M. Attamimi, "Object extraction using probabilistic maps of color, depth, and near-infrared information," *JAREE (Journal on Advanced Research in Electrical Engineering)*, vol. 4, no. 1, Apr. 2020, doi: 10.12962/j25796216.v4.i1.106.
- [66] F. Xue, S. Xu, Y.-T. Luo, and W. Jia, "Design of digital camouflage by recursive overlapping of pattern templates," *Neurocomputing*, vol. 172, pp. 262–270, Jan. 2016, doi: 10.1016/j.neucom.2014.12.108.
- [67] M. J. Swain and D. H. Ballard, "Color indexing," *International Journal of Computer Vision*, vol. 7, no. 1, pp. 11–32, Nov. 1991, doi: 10.1007/BF00130487.
- [68] H. Akima, "A method of bivariate interpolation and smooth surface fitting for irregularly distributed data points," *ACM Transactions on Mathematical Software*, vol. 4, no. 2, pp. 148–159, Jun. 1978, doi: 10.1145/355780.355786.
- [69] J. Aschoff, "Circadian rhythms: influences of internal and external factors on the period measured in constant conditions1," *Zeitschrift für Tierpsychologie*, vol. 49, no. 3, pp. 225–249, Apr. 1979, doi: 10.1111/j.1439-0310.1979.tb00290.x.





- [70] G. S. Choi, S. W. Kang, E. J. Bae, B.-K. Ju, and Y. W. Park, "A morphological study of random nanostructured external light extraction layers for enhancing optical characteristics of OLEDs," *Journal of Materials Chemistry C*, vol. 11, no. 41, pp. 14307–14315, 2023, doi: 10.1039/D3TC02334F.
- [71] G. H. Beckman, D. Polyzois, and Y.-J. Cha, "Deep learning-based automatic volumetric damage quantification using depth camera," *Automation in Construction*, vol. 99, pp. 114–124, Mar. 2019, doi: 10.1016/j.autcon.2018.12.006.

BIOGRAPHIES OF AUTHORS







Bernadeta Siti Rahayu Purwanti     is Associate Professor at the Department of Electronics Engineering, State Jakarta of Polytechnic, Depok, Indonesia. She received the B.Sc. degree in electrical engineering from Universitas Diponegoro, Semarang, Indonesia and the M.Sc. degree from Universitas Indonesia. Her research areas are image/signal processing, pattern recognition, and digital feature extraction. She can be contacted at email: rahayu.purwanti@elektro.pnj.ac.id.







Ihsan Auditia Akhinov     received the bachelor of engineering (S.T.) degree in Electrical Engineering from Universitas Andalas, Padang, Indonesia, and the Master of Engineering (M.T.) degree in Electrical Engineering from Institut Teknologi Bandung (ITB), Bandung, Indonesia. His research interests include microprocessor, image processing, instrumentation, automation system, and artificial intelligence. He can be contacted at email: ihsan.auditia.akhinov@elektro.pnj.ac.id.







Raden Sugeng Mulyono     is Associate Professor at the Department of Mechanical Engineering, Politeknik Negeri Jakarta, Jakarta, Indonesia. He received the bachelor's degree in Electrical Engineering from Universitas Negeri Yogyakarta (UNY), Yogyakarta, Indonesia and Universitas Indonesia and master's degree in Computer Science (Management Information System). His research area in CAD, engineering drawings, machine elements, pneumatic/hydraulics, autocad, and mechanical design techniques. He can be contacted at email: sugeng.mulyono@mesin.pnj.ac.id.



Assoc. Prof. Dr. Ir. Muhammad Nurtanto, M.Pd     is an assistant professor in Department of Mechanical Engineering, Jakarta State Polytechnic, Demak, Indonesia. Research interests in the fields of professional learning, teacher emotion, teacher identity philosophy of education, STEM education, gamification, and teacher quality in vocational education. He can be contacted at email: muhammad.nurtanto@mesin.pnj.ac.id.



Assoc. Prof. Mustofa Abi Hamid     (Member, IEEE), is a doctoral student at Graduate School of Technological and Vocational Education, Universitas Negeri Yogyakarta. He is also an Associate Professor of Technical and Vocational Education and Training (TVET) at the Department of Electrical Engineering Vocational Education, Universitas Sultan Ageng Tirtayasa. He has written several papers in the areas of technical and vocational education and training, digital learning, e-learning, evaluation of learning, learning media, ICT for learning. His research interests also include learning strategies, pedagogical innovations in TVET, skills and personal development, and innovations in engineering and education. He is member of Asian Academic Society for Vocational Education and Training (AASVET), member of European Research Network Vocational Education and Training (VETNET), and member of IEEE Education Society. At the national level he serves as assessor of National Accreditation Board for Early Childhood, Primary and Secondary Education for the Ministry of Education and Culture of Republic of Indonesia since 2020 until now. He can be contacted at email: abi.mustofa@untirta.ac.id; mustofa@ieee.org; and mustofaabi.2023@student.uny.ac.id.